View metadata, citation and similar papers at core.ac.uk

brought to you by CORE

provided by NASA Technical Reports Server

Quarterly Progress Report

For Period

April 1 - June 30, 1966

FUNDAMENTAL STUDIES OF THE METALLURGICAL, ELECTRICAL, AND OPTICAL PROPERTIES OF GALLIUM PHOSPHIDE

GPO PRICE $ _____

CFSTI PRICE(S) $ _____

Hard copy (HC) $2.00

Microfiche (MF) .50

#853 July 65

Grant No. NsG-555

Prepared For

NATIONAL AERONAUTICS AND SPACE ADMINISTRATION
LEWIS RESEARCH CENTER
CLEVELAND, OHIO

Work Performed By

Solid-State Electronics Laboratories
Stanford University
Stanford, California

FACILITY FORM 602

N66 31373 (ACCESSION NUMBER) (THRU)

28 (PAGES) 1 (CODE)

CR-76395 (NASA CR OR TMX OR AD NUMBER) 26 (CATEGORY)

PROJECT 5109: EPITAXIAL GROWTH OF III-V SEMICONDUCTOR COMPOUNDS

National Aeronautics and Space Administration
Grant NsG-555
Project Leader: G. L. Pearson
Staff: D. H. Loescher*

The purpose of this project is to study the chemical, electrical and optical properties of cobalt as an impurity in gallium phosphide. The thermodynamic properties of ternary systems consisting of GaAs or GaP and an added impurity are also under investigation.

I. Introduction

The study of cobalt doped gallium phosphide naturally divides itself into three parts, namely: (1) the metallurgical properties of the cobalt-gallium - phosphorus ternary system; (2) the electrical properties of cobalt doped gallium phosphide crystals; (3) the optical properties of cobalt doped crystals. The discussion below summarizes our work during the past quarter on parts (1) and (2).

II. Experiement

Hall effect and resistivity measurements were made on a number of samples of cobalt doped GaP. The details of the sample preparation and of the electronic measuring equipment were given in the last quarterly report (Ref. 1).

III. Result

The results of the electrical measurements are summarized in Fig. 1. The data points are from two samples, CS1, and CS2, each of which contained 6×10^{16} cm^{-3} sulfur and 9×10^{16} cm^{-3} cobalt. The sign of the Hall coefficient showed that the samples were p-type.

*NSF Fellow

The hole mobility calculated from the CS1 and CS2 data is shown in Fig. 2.

IV. Discussion

The ionization energy of cobalt acceptors is 0.41 eV +0.02 eV. This value is calculated from the slopes of the plots shown in Fig. 1.

The following arguments will show why the cobalt impurity cannot be treated as a shallow impurity. The theory of shallow impurities results from expanding the impurity wave function in terms of Bloch waves. This expansion is not practical when the impurity wave function occupies only a very small volume of the crystal. A very small orbit is in some ways analogous to an impulse in that both require a large number of terms in their Fourier expansion: a Bloch wave expansion is essentially the same as the Fourier expansion. So to see if the Bloch expansion can be used we must estimate the size of the impurity orbit. This can be done by using the Bohr theory of the atom to find the radius of the 0.41 eV orbit. Such an estimate places the radius between 2 and 20Å. These values of the radius correspond to localizing the electron into 16 or fewer unit cells. Since localizing the electron this much would require a nearly infinite Bloch wave expansion, such an expansion and hence the theory of shallow impurities cannot be applied to the cobalt level

V. Conclusions

An acceptor level 0.41 eV above the valence band has been attributed to cobalt doping. No other level that could be

attributed to cobalt was seen in the measurements. It was shown that the theory of shallow impurities could not be applied to the cobalt level.

A final report on this project is being prepared and should be ready for distribution in the fall.

REFERENCES

1. D. H. Loescher, Quarterly Progress Report, Grant NsG-555, January 1 to March 31, 1966.

FIGURE TITLES

1. Hall Coefficient and Resistivity as a Function of Reciprocal Temperature for Cobalt Doped Samples CS 1(o) and CS 2(x).

2. Hole Mobility versus Temperature In Samples CS 1(o) and CS 2(x).

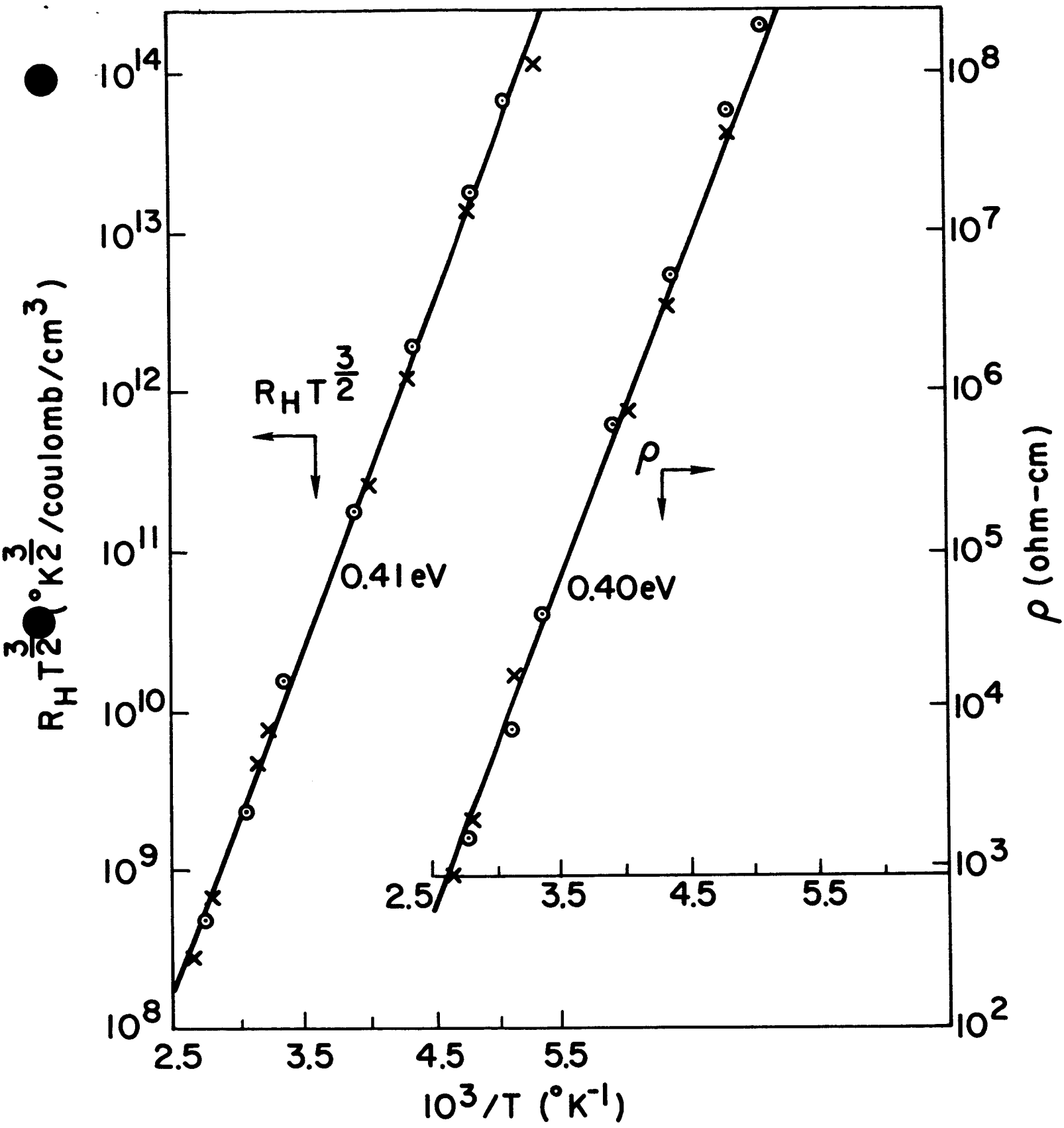
10^{14}
10^{13}
10^{12}
10^{11}
10^{10}
10^{9}
10^{8}
$R_H T^{\frac{3}{2}}$
0.41 eV
0.40eV
ρ
2.5
3.5
4.5
5.5
$10^{3}/T\ (°K^{-1})$
$R_H T^{\frac{3}{2}}\ (°K^{\frac{3}{2}}\text{coulomb/cm}^3)$
10^{8}
10^{7}
10^{6}
10^{5}
10^{4}
10^{3}
10^{2}
ρ (ohm-cm)

FIG. 1

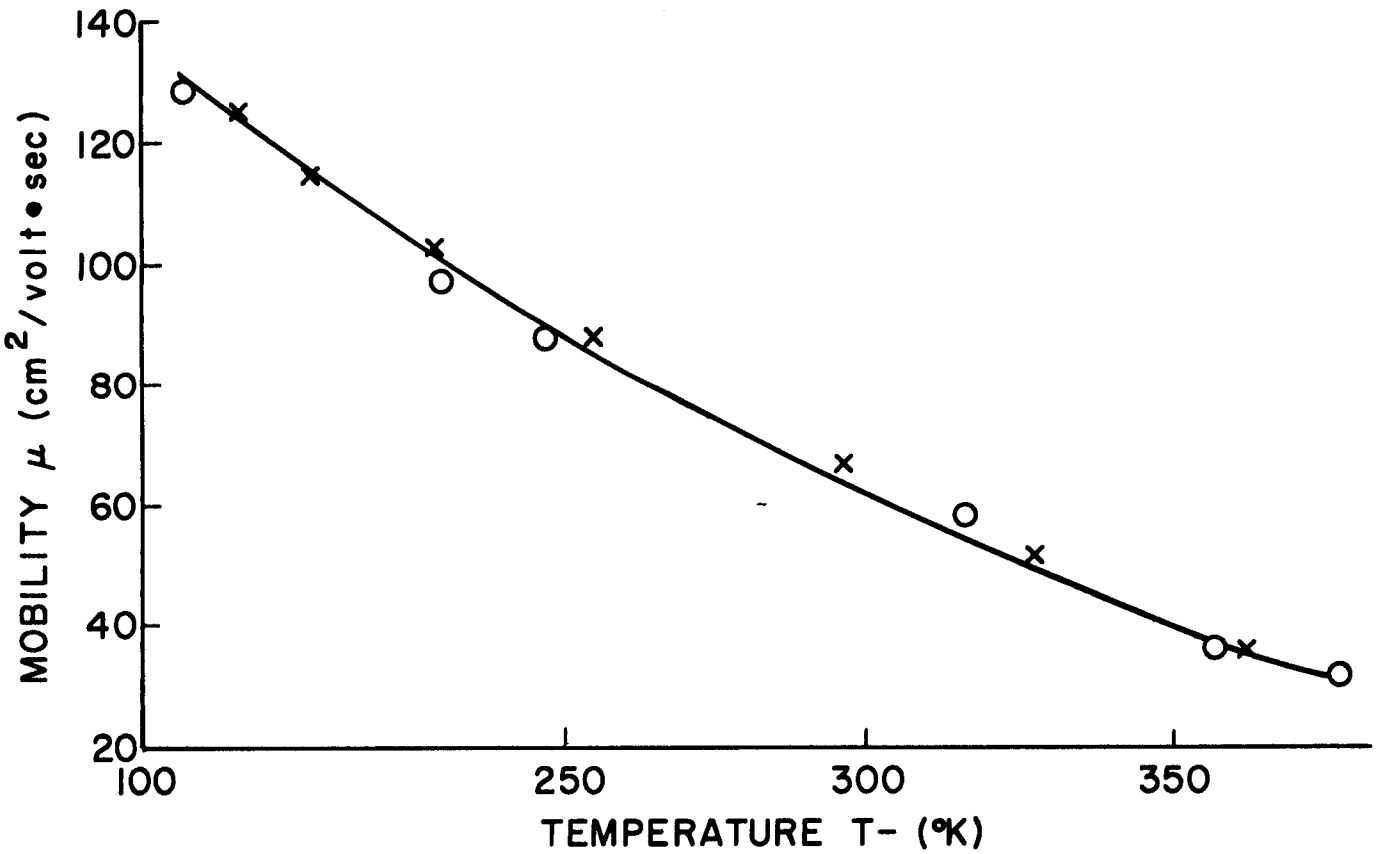
140
120
100
80
60
40
20
MOBILITY μ (cm²/volt • sec)
100
250
300
350
TEMPERATURE T- (°K)

FIG. 2

PROJECT 5112: THE PROPERTIES OF RECTIFYING JUNCTIONS IN $GaAs_xP_{1-x}$

National Aeronautics and Space Administration
Grant NsG-555
Project Leader: G. L. Pearson
Staff: S. F. Nygren*

The purpose of this project is to study the preparation and characterization of rectifying junctions in GaP and $GaAs_xP_{1-x}$. In particular, we wish to relate the structure of the crystals to the electrical properties of the junctions. During the quarter our investigations have included further study of the imperfections in the GaP crystals grown in this Laboratory, a look at the diffusion front when zinc is diffused into GaP, and a characterization of two solar cells that were made from GaP crystals grown in this Laboratory.

A. Imperfections in Gallium Phosphide Crystal

We have made a study of the etch pit patterns produced on crystals C1, C3, and C4 by etchant #1 [8 $K_3Fe(CN)_6$: 12 KOH : 100 H_2O]. Crystals C1 and C3 had been grown epitaxially on a {111} Ga face of a GaAs substrate by the method usually used in this Laboratory. Crystal C4 had been grown by the same method except that it was grown on a {111} As face of the substrate. [Ref. 1]

Number 600 grit bonded to a rubber wheel was used to cross section crystal C1 in such a way as to expose a {111} plane other than the growth plane. Etchant #1 revealed many planar imperfections in the cross section. It also revealed that the dislocation density was not uniform. There was a high concentration of etch pits near the face of C1 that had been attached to the substrate. This was

*NSF Fellow

followed by a layer with fewer etch pits, another layer with more, and still another with fewer.

Crystal C3 was first etched to demonstrate conclusively that large etch pits form most clearly on the {111} Ga face of the crystal; not the {111} P face as stated previously.[Ref. 2] The etch patterns on crystal C3 also revealed a high density of both dislocations and planar imperfections. The dislocation density was about 3×10^{5} cm^{-2}.

Crystal C4 was expected to be quite imperfect. It had been grown at a temperature that would have been proper for growth on a {111} Ga face of a substrate, but which may have been wrong for growth on a {111} As face of a substrate. The growth surface of C4 was quite rough. When etchant #1 was used on a small chip of crystal C4 that had been lapped smooth with 3200 grit, two distincly different regions of etch patterns developed, suggesting polycrystallinity. Indeed, when the Monsanto Company examined another piece of the same crystal, they concluded that it "was highly twinned and contained a considerable amount of grosser polycrystallinity."

B. Diffusion of Zinc Into Gallium Phosphide

Zinc was diffused into GaP crystal C1 so that we could see the effects of planar imperfections and dislocations on diffusion. A piece of crystal C1, 0.04 cm thick and with {111} faces 0.2 cm by 0.4 cm, was lapped smooth with 3200 grit. The piece of crystal and 0.1 mg of zinc were placed inside a quartz tube with 0.3 cm inside diameter. The tube was evacuated to a pressure of 1×10^{-3} mm of Hg. Then the 1.1 cm long section containing the crystal and the zinc was sealed, forming a diffusion ampoule.

The ampoule was placed in a furnace, and diffusion was allowed to proceed for 15 minutes at 1000°C. Then the ampoule was quickly withdrawn from the furnace and dropped onto the metal track in front of the furnace, quenching the diffusion. The ampoule was opened and the crystal was cleaved to expose a {110} cross section. The crystal was then placed in boiling aqua regia for one minute to reveal the diffusion front on the cleaved surface and to produce etch patterns on the {111} surfaces.

Figures 1 and 2 show examples of the diffusion front. The front is clearly not planar; on the average it is about 4.5 μm from the surface, but it has many spikes which seem to have been caused by diffusion short circuits. Several of these spikes have straight lines running from the tip of the spike to the surface of the crystal. The angle between one of these lines and the surface is always either 55° or 70°. These angles are those that would be made by the intersections of the traces of {111} planes on a {110} surface.

Figure 2 and 3 show that there is a correlation between the planar imperfections revealed on the surface of the crystal and the spikes in the diffusion front. The lines of etch pits marking the planar imperfections on the {111} surface of the crystal [Fig. 3] intersect at angles of 120° and 60°. These angles are those that would be made by the intersections of the traces of {111} planes on a {111} surface. Thus we conclude that the diffusion short circuits are planar imperfections parallel to {111} planes.

Chang and Pearson [Ref. 3] have demonstrated that zinc diffuses into GaP by the parallel mechanisms of interstitial and substitutional diffusion. Because of this parallel mechanism, the diffusion rate is slowed down when excess phosphorus is present during diffusion. Our future work will include several diffusions done at different phosphorus pressures to see what effect phosphorus pressure has on the spikes in the diffusion front.

C. Gallium Phosphide Solar Cells

We have studied two GaP solar cells that were fabricated from crystals grown in this laboratory. The crystals were sulfur doped with Cell 11 having $n = 6 \times 10^{16}$ cm^{-3}, and Cell 21 having $n = 1 \times 10^{18}$ cm^{-3}. Electro-Nuclear Corporation, Mountain View, California, diffused zinc into these crystals from a $ZnAs_2$ source for 20 minutes at 850°C. This was calculated by them to give a junction depth of 6 μm. After diffusion, they removed the diffused layer from one side of each crystal, scribed and cleaned them, and etched them in aqua regia. They applied contacts: to the n side, a layer of 50% Au - 50% Sn followed by a layer of pure Au; to the p side, a layer of 99% In - 1% Zn. All contacts were alloyed at 550°C. The solar cells were then mounted on TO-5 headers. The area of Cell 11 was 6.8×10^{-2} cm^2; Cell 21 was 6.2×10^{-2} cm^2.

In the dark, both cells have similar current-voltage characteristics. In the forward direction, for 0.1 v < V < 1.7 v, both have currents which obey $I = I_o e^{\frac{qV}{nkT}}$ only if we allow n to be a function of voltage. For low voltages n is about 4. It increases to almost 9 as voltage increases. Then, as the voltage approaches

1.7v, n decreases to about 4 again. This result is similar to Koike's [Ref. 4]

The short circuit current spectral response is shown in Figure 4. A monochromatic beam of light from a Bausch and Lomb monochromator, was shined directly on a solar cell. An HP 425 A microvolt-ammeter was used to measure the short circuit current of the cell. When needed, an optical filter was placed in the light path to remove second order radiation. The response curve was corrected for the emission spectrum of the light source and for any nonlinearities the monochromator might have. Then the curves were normalized so that the peak of each curve was given a value of unity.

Each spectral response curve may be explained qualitatively by saying that it is the product of two curves. The first curve gives the response that the cell would have if all of the light were absorbed at the p-n junction. It would be zero for photon energies from zero to about 2.24 e.V. (since the band gap of GaP is 2.24 e.V. at room temperature), and then it would begin to rise with increasing photon energy as more and more allowed transitions become available. This curve would eventually saturate when the photon energy became sufficiently large to excite any electron from the valence band into any state in the conduction band.

The second curve gives the amount of light that is actually absorbed within one diffusion length of the depletion region. The intensity, I, of light travelling through the crystal decreases as

$$I = I_o \exp(-\alpha x)$$

where I_o is the intensity of light at the surface where $x = 0$, and α is the absorption coefficient. Since α increases abruptly when the photon energy reaches the energy of the direct gap in GaP (estimated by various workers to be between 2.6 eV and 2.8 eV), the amount of light reaching the junction decreases abruptly at that value of energy. Thus the spectral response curve is the product of one curve that begins to rise at about 2.24 eV and a second which drops sharply at about 2.7 eV.

The fact that light travelling through the crystal is attenuated exponentially with distance means that more light will be absorbed in the region of the junction if the junction is near the surface. This is particularly true for ultraviolet radiation where the absorption coefficient is high. Putting the junction close to the surface will, however, increase the series resistance of the cell, impairing its performance somewhat.

The power curve is plotted in Figure 5. For this measurement, the solar cells were placed in direct sunlight which may be assumed to have a power of about 10^{-1} watts/cm^2. Under this assumption both cells are about 0.1% efficient.

Future work in this area will consist of making several more cells and investigating their responses as functions of junction depth and donor concentration in the n region.

REFERENCES

1. S. F. Nygren, Quarterly Progress Report for Period January 1 - March 31, 1966.

2. S. F. Nygren, SEL Quarterly Research Review No. 15.

3. L. L. Chang and G. L. Pearson, "Diffusion Mechanism of Zn in GaAs and GaP Based on Isoconcentration Experiments," J.A.P. 35, 1960 (1964).

4. T. Koike, SEL Quarterly Research Review No. 14.

FIGURE TITLES

Fig. 1 A {110} Cross-Section of Crystal C1 After Diffusion and Etching.

Fig. 2 Another Region of the {110} Cross Section of C1.

Fig. 3 The {111} Surface of Crystal C1. This is the same Section of the Crystal as shown in Figure 2.

Fig. 4 Spectral Response of Relative Short Circuit Current of Solar Cells 11 and 21.

Fig. 5 Output Current and Voltage for Solar Cells 11 and 21 Under Sunlight.

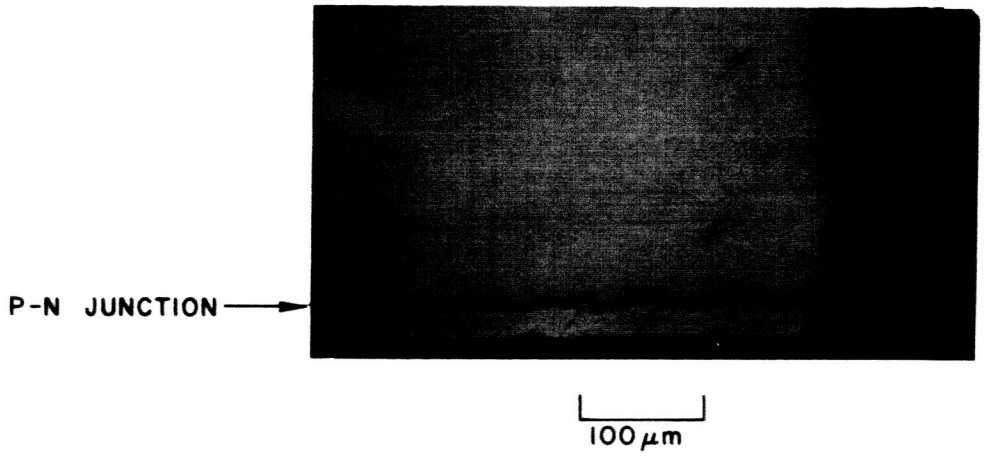

FIG. 1

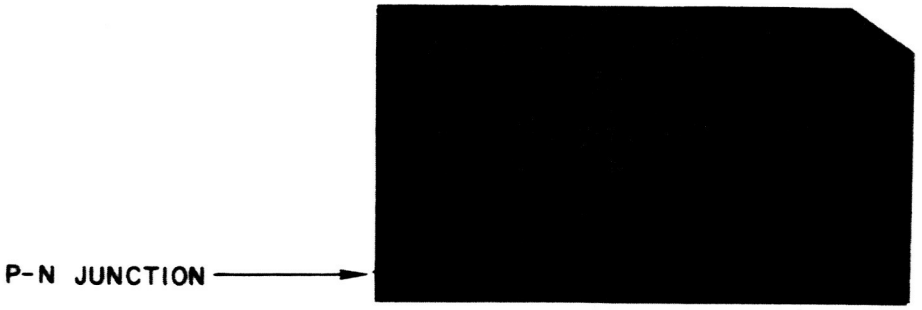

FIG. 2

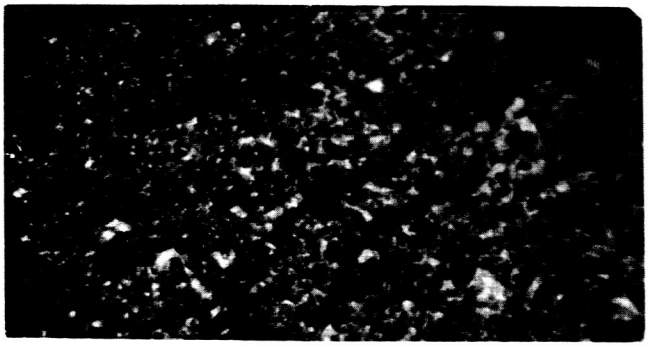

FIG. 3

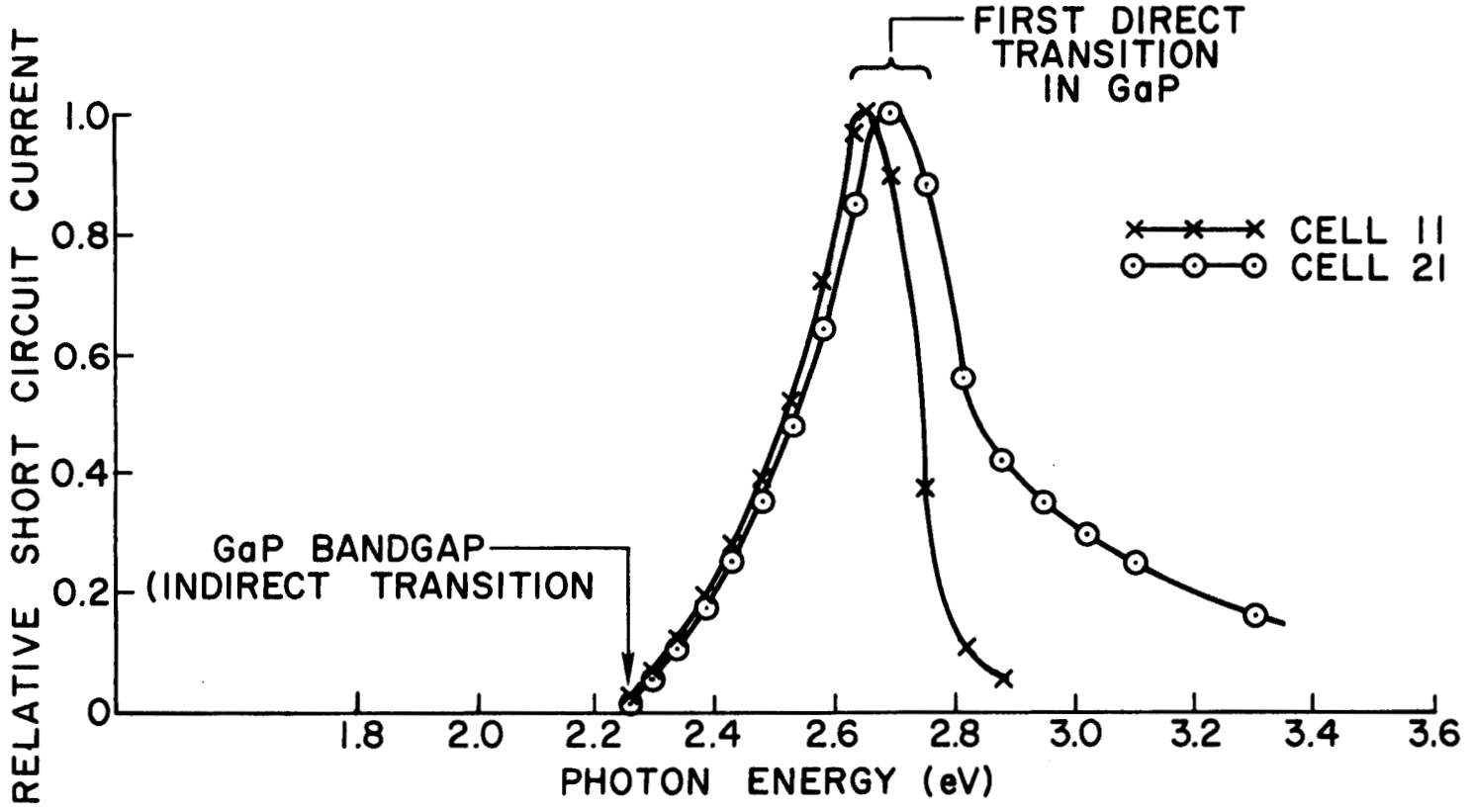
FIRST DIRECT
TRANSITION
IN GaP
CELL 11
CELL 21
GaP BANDGAP
(INDIRECT TRANSITION
RELATIVE SHORT CIRCUIT CURRENT
1.0
0.8
0.6
0.4
0.2
0
1.8
2.0
2.2
2.4
2.6
2.8
3.0
3.2
3.4
3.6
PHOTON ENERGY (eV)

FIG. 4

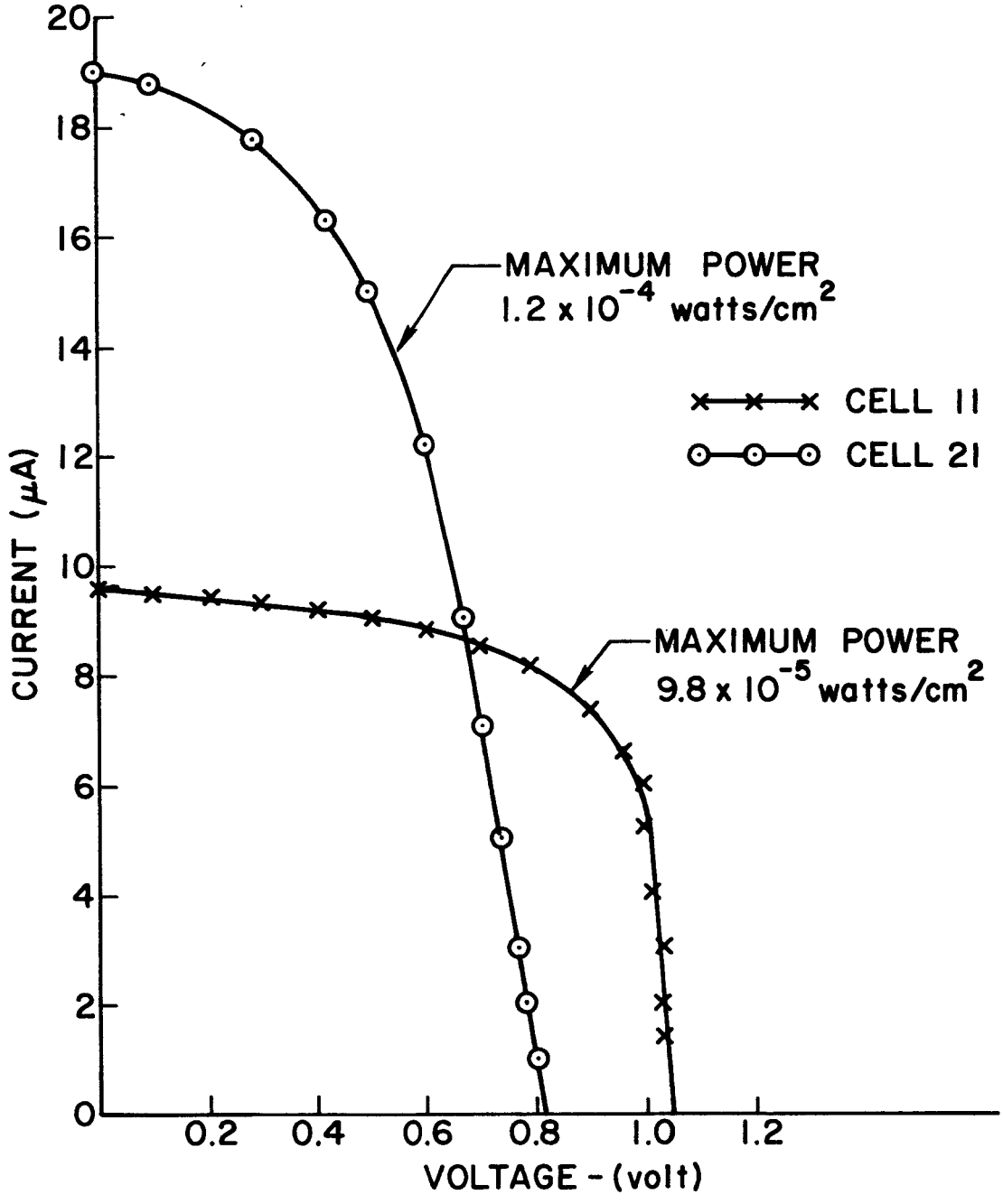
20
18
16
14
12
10
8
6
4
2
0
CURRENT (μA)
0.2
0.4
0.6
0.8
1.0
1.2
VOLTAGE - (volt)
MAXIMUM POWER
1.2 x 10^-4 watts/cm^2
CELL 11
CELL 21
MAXIMUM POWER
9.8 x 10^-5 watts/cm^2

FIG. 5

PROJECT 5115: SEMICONDUCTING PROPERTIES OF GALLIUM PHOSPHIDE

National Aeronautics and Space Administration
Grant NsG-555
Project Leader: G. L. Pearson
Staff: J. W. Allen

The purpose of this project is to study the properties of GaP and $GaAs_xP_{1-x}$ relevant to their use as semiconducting materials.

In previous reports we have developed a theoretical and experimental treatment of a particular kind of deep impurity in semiconductors, the kind in which there is an incomplete electron shell. Optical absorption due to transitions within the shell gives us information concerning the electron configuration and lattice site of the impurity. A simple semi-empirical model explains the positions of the impurity energy levels with respect to the valence and conduction bands and allows some predictions to be made concerning unknown levels. In this last quarter we have given some consideration to the problem of optical transitions from the impurity to a conduction or valence band. Although these transitions are of great technical importance, as for instance in photoconductivity, there exists as yet no theory of such things as the excitation spectrum or the strength of the transition.

Consider a transition in which the impurity has a configuration d^n in the initial state and d^{n-1} in the final state. (The theory also holds for f^n configurations.) The electric dipole is represented by a one-electron operator so there is a selection rule that the transition matrices will only involve single orbital changes. We therefore need only consider terms of the type

$$\langle d^n S\Gamma | \underline{r} | d^{n-1} S'\Gamma' . {}^{vb}_{cb} \rangle \qquad (1)$$

where S,Γ are spin and symmetry labels and vb,cb stand for a valence band or conduction band state respectively. It is possible to uncouple a d-orbital from the d^n configuration by using the idea of fractional parentage. Tabulations of the relevant coefficients are given for example by Griffith[1] or by Nielson and Koster.[2] By this means the elements of Eq. (1) can be reduced to terms of the form

$$\langle d|\underset{\sim}{r}|{}^{vb}_{cb}\rangle \quad . \tag{2}$$

To illustrate the behaviour of these terms we consider a tight-binding model of a semiconductor with band extrema at the centre of the Brillouin zone, as for example the II-VI compounds. In these the top of the valence band is made up predominantly of atomic p-orbitals and the matrix elements (2) correspond to allowed transitions. The optical spectrum will then reflect the density of states and will have the form

$$\begin{cases} (\nu - \nu_o)^{1/2} & \nu > \nu_o \\ 0 & \nu < \nu_o \end{cases} \tag{3}$$

where $h\nu_o$ is the energy of the separation of the impurity from the valence band. At higher energies the absorption will contain extra terms corresponding to the impurity ending in an excited state.

The conduction band is made up of s-orbitals near the minimum so transitions are parity-forbidden. Two effects then come into play. As one goes up the conduction band p-like behaviour occurs. The magnitude of this contribution could be estimated for instance by a $\underset{\sim}{k} \cdot \underset{\sim}{p}$ procedure. There will be a gradually increasing contribution to the intensity as energy increases. In addition, if the lattice site of the impurity lacks

inversion symmetry, as in the zinc-blende or wurtzite structures, then parity will not be a good quantum number for the impurity orbitals. We may write the t_2-orbitals in the form

$$\cos\theta|t_2(d)\rangle + \sin\theta|t_2(p)\rangle \qquad (4)$$

where θ is a small angle, describing mixing of valence band and impurity orbitals. The odd parity part will then have a non-zero interaction with the s-like conduction band. In order to evaluate this contribution it is necessary to estimate θ, which can be done in principle by using the measured oscillator strengths for transitions within the d-shell.

The ground-work of the theory has now been laid, and we can procede to build on it. For the experimentalist, the upshot of all this is as follows. Optical transitions from the valence band of a II-VI or III-V semiconductor to a transition metal impurity will be strong and have a simple spectrum with a reasonably well-defined threshold corresponding to the energy level of the impurity. Transitions to the conduction band will have a form which consists of the addition of a number of terms and will be weak in the threshold region. Empirical extrapolation to a threshold energy in order to obtain the impurity energy level may be an unreliable procedure.

References

1. J.S. Griffith. "Theory of Transition-Metal Ions." (Cambridge University Press, 1961).

2. C.W. Nielson and G.F. Koster. "Spectroscopic Coefficients for p^n, d^n and f^n Configurations." (MIT Press, 1964).

PROJECT 5116: DONOR IMPURITIES IN GaP

National Aeronautics and Space Administration
Grant NsG-555
Principal Investigator: G. L. Pearson
Staff: A. Young*

The purpose of this project is to study the behavior of shallow donors in gallium phosphide. In particular, S, Se, and Te will be diffused into GaP to determine solubilities and diffusion parameters. This information will be useful in delineating the properties of GaP doped with these shallow donor impurities.

The first step will be a radiotracer experiment with S^{35} being diffused into GaP. From this work we hope to map out the solidus curve (or at least that portion of the region without excessive pressures) and the details of the diffusion process; that is the diffusion profile and the diffusion constant. These data will be valuable in the fabrication of devices doped with sulfur by diffusion.

The solidus region of a ternary system may be mapped as shown in Fig. 1 for the Ga-As-Zn system.[1] This diagram shows the region of the stability of zinc doped GaAs in terms of the zinc and arsenic pressures. (The diagram is a schematic only and no numbers are given.) The ternary systems being studied are of particular interest because the solidus region is expected to be quite extensive with high donor solubilities in the host GaP lattice.

Radautsan and Negreskul[2] have reported on solid solutions of GaP and Ga_2S_3 which were formed by fusing the two components under vibration mixing. Quite high solubilities were found. For the system $(Ga_3P_3)_x\ (Ga_2S_3)_{1-x}$, solid solutions were reported from

*NSF Fellow

100% Ga_3P_3 (x = 1) to 30% Ga_3P_3 (x = 0.3)[2]. It was suggested that the solubility may be even higher under more optimum conditions. For the case reported by these workers, the concentration of sulfur atoms is roughly 1.7×10^{22} or a third of the total atoms in the crystal.

Previous attempts to dope GaAs heavily with sulfur have resulted in the formation of a GaS phase at the surface.[3] We hope to avoid this difficulty in GaP by working within the solidus boundary with a proper choice of sulfur and phosphorus pressures.

The electrical properties of sulfur doped GaP should be quite interesting since, while GaP lightly doped with sulfur is n-type, Ga_2S_3 lightly doped with P is expected to be p-type. Similar studies of this transition region in the Ga-As-Se system have been carried out by Vieland and Kudman.[4]

Our work with Se and Te in GaP is expected to follow the same procedures as that being done with sulfur.

Experimental

During the last quarter 3 undoped GaP crystals were grown by the open tube method developed by Chen and Loescher in this laboratory.[5] Resistivity and mobility measurements on these crystals using the Van de Pauw method yielded the results shown in Table 1. (Sigh of the mobile carriers has not yet been determined.) Planning of the radiotracer experiment is proceeding, and diffusions will be started next quarter.

Crystal No.	Resistivity (ohm-cm)	Hall Mobility (cm^2/v-sec)	Carrier Concentration (cm^{-3})
1	23.6	96	2.8×10^{15}
2	7.9	112	7×10^{15}
3	24.8	60	5×10^{15}

TABLE 1

Resistivity and Mobility of Undoped GaP Crystals Grown During This Quarter

REFERENCES

1. J. W. Allen and G. L. Pearson, Stanford TR 5109-1, May 1965 p. 19.

2. S. I. Radautsan and V. V. Negreskul, Soviet Research in New Semiconductor Materials, 1965, p. 104.

3. B. Goldstein, Phys. Rev. 121, 1305 (1961).

4. L. J. Vieland and I. Kudman, J. Phys. Chem. Solids, 24, 437, (1963).

5. Y. S. Chen, SEL QRR Nos. 10, 11.
   D. Loescher, SEL QRR Nos. 12, 14.

FIGURE TITLES

Fig. 1 Solidus Region of the Ga-As-Zn System (Schematic Only).

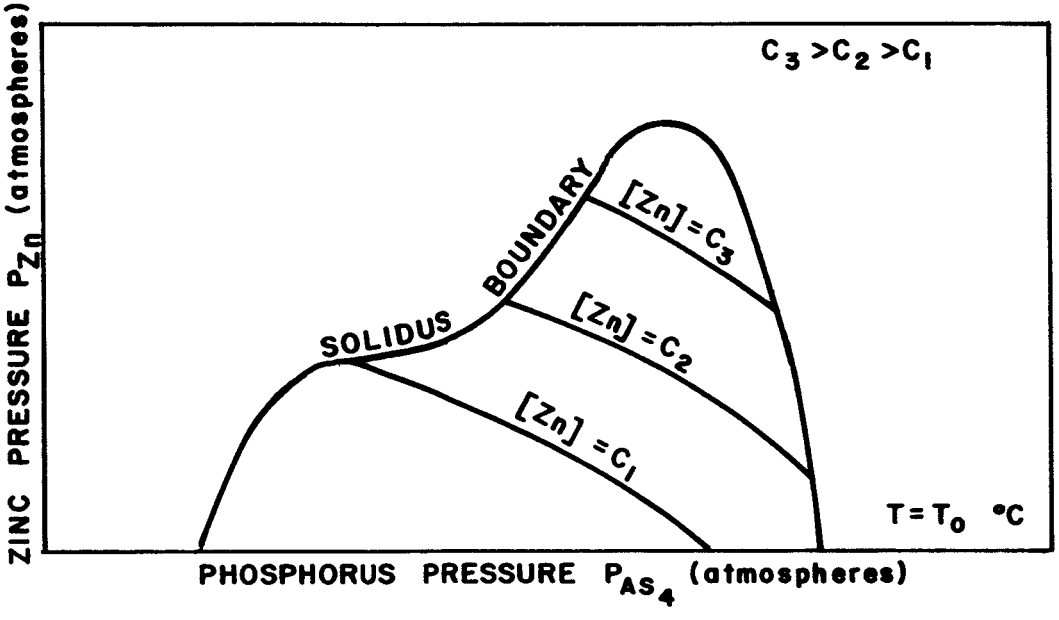
$C_3 > C_2 > C_1$
BOUNDARY
SOLIDUS
[Zn] = C_3
[Zn] = C_2
[Zn] = C_1
T = T_0 °C
ZINC PRESSURE P_{Zn} (atmospheres)
PHOSPHORUS PRESSURE P_{AS_4} (atmospheres)

FIG. 1